

Impacts of EPS inclusion density and backfill soil type on earth pressure reduction around a buried pipe

Alan F. Witthoeft

Geo-Logic Associates, Inc., USA

Hobi Kim

Daelim Industrial, Co., Ltd., Korea

Dongwook Kim

Incheon National University, Korea

ABSTRACT: Expanded Polystyrene (EPS) geofoam compressible inclusions placed over buried pipes are effective in reducing the earth pressure due to positive arching action. However, practical guidance for design is sparse. In particular, there is a scarcity of studies considering the influence of soil type and EPS density, individually and in combination, on compressible inclusion performance and optimal dimensions. This paper presents a finite difference method-based (using FLAC software) study of the effects of soil type and EPS density on the pressure distribution around a buried pipe. Tentative recommendations are also provided for buried pipe design when using an EPS inclusion. Numerical analyses were performed for different combinations of three soil types and three EPS densities. The numerical results show that the effectiveness of the EPS compressible inclusion can be predicted with a reasonable degree of accuracy based on the relationship between the soil and EPS stiffnesses. An *effective compressibility index* is proposed as an indicator to predict reduction of overburden stress on the pipe based on the soil stiffness and the EPS panel compressibility.

Keywords: *Geosynthetics, Buried pipes, Compressible inclusion, EPS (expanded polystyrene) geofoam, Imperfect ditch condition, Numerical study*

1 INTRODUCTION

Use of a compressible inclusion over a buried pipe is one method to reduce earth loads acting on the pipe and, thereby, to reduce the required capacity of the design pipe section. This approach, which has been discussed by several authors since Marston (1930), can be a useful means of generating cost savings for pipe or culvert installations below high fills. For example, AbdelSalam and Azzam (2016) characterized mechanical properties of geofoam materials and examined behavior of rigid and flexible walls with geofoam implementation numerically. The authors found significant reduction of lateral pressure on flexible walls. Athanasopoulos et al. (1999) conducted torsional resonant column tests and cyclic uniaxial tests on block-molded expanded polystyrene (EPS) geofoam specimens to investigate their dynamic properties. It was found that the dynamic properties of EPS geofoam were governed by the EPS geofoam density.

Previous studies, including those by Horvath (1997), Bartlett and Lingwall (2014), Kim et al. (2010), and Witthoeft and Kim (2016), have investigated the effects of variation of compressible inclusion geometry on earth pressure around a pipe. These experimental and numerical studies include evaluation of earth pressure reduction on a laboratory-scale buried pipe for different compressible inclusion configurations (i.e., various compressible inclusion widths and thicknesses) and evaluation of the use of a stacked panel configuration (i.e., using two panels spaced vertically above the pipe). However, the laboratory-scale studies of Kim et al. (2010) and Witthoeft and Kim (2016) were conducted for limited cases as follows: (i) Only one soil [Jumunjin sand, which is poorly graded sand (SP)] with constant relative density of approximately 44% was considered; and (ii) only one EPS type with a density of approximately 15 kg/m³ was considered.

The purpose of this numerical study is to expand upon the previous work of Kim et al. (2010) and Witthoeft and Kim (2016). In particular, this study considers three soil types (i.e., well-graded sands and

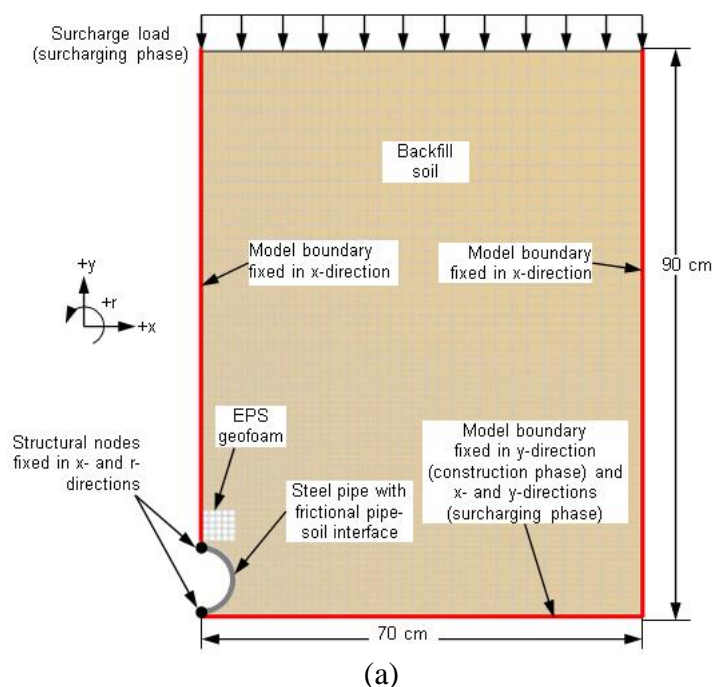
gravelly sands, SW; inorganic silts or very fine sands, ML; and inorganic clays of low to medium plasticity, CL) and three EPS types (i.e., EPS12, EPS15, and EPS19). Soil properties were assumed based on Boscardin et al. (1990) parameter sets for corresponding classifications (i.e., SW, ML, and CL) at 95% standard Proctor density. EPS properties were assumed based on standard EPS classifications (i.e., densities) listed in ASTM D6817M-15 (ASTM, 2015) and density-dependent parameter values based on Kim et al. (2018). Based on results of the parametric study, this paper presents a relationship between relative stiffness (i.e., the ratio of soil to EPS constrained modulus values) of the soil and EPS and the reduction in overburden stress. This relative stiffness approach, which is substantially independent of soil type *per se*, can be used to generate preliminary estimates of the degree of overburden stress reduction for a given combination of soil stiffness and compressible inclusion characteristics.

2 MODEL GEOMETRY AND MATERIAL PROPERTIES

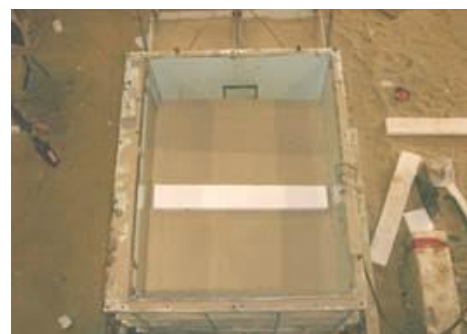
2.1 Model Geometry and Boundary Conditions

A plane-strain model was developed using FLAC software (Itasca, 2011). The model geometry and loading sequence were based on those used by Witthoeft and Kim (2016) to simulate the Kim et al. (2010) laboratory scale tests, although the magnitude of the final surcharge load and the far-field boundary condition (i.e., the vertical boundary along the test box wall away from the pipe) were changed to approximate an infinitely wide fill embankment. Due to symmetry, only half of the test box was included in the simulation. The geometry and boundary conditions of the numerical model and pictures of experimental model are shown in Figure 1.

Each simulation was separated into two phases: a construction phase and a surcharging phase. The construction phase consisted of a sequence in which one row of numerical zones at a time was activated (for a soil lift thickness ranging from approximately 10 mm to 33 mm) and the model was allowed to reach static equilibrium. Rows of numerical zones were activated sequentially from the bottom of the model to the top of the model. During the surcharging phase, a vertical stress boundary condition was applied along the top of the model. The magnitude of this vertical stress was increased in increments of 1 kPa, allowing the model to equilibrate between increments, until reaching the maximum applied surcharge load of 150 kPa.



(b)



(c)

Figure 1. FLAC model: (a) geometry and boundary condition, (b) front view and (c) upper view of experimental model

Displacement constraints were applied as shown in Figure 1. Horizontal displacement constraints were used along the plane of symmetry and along the right model boundary. The lateral and rotational degrees of freedom were fixed for the structural nodes lying on this boundary at all stages of the analyses. The lower boundary was fixed in the vertical direction during the construction phase and was fixed in both horizontal and vertical directions during the surcharging phase.

Pipe-soil interaction was modeled as a frictional interface using the FLAC software’s built-in interface logic. Interface properties developed by Witthoeft and Kim (2016) were used. EPS-soil interaction was modeled assuming a no-slip condition. Based on preliminary simulations reported by Witthoeft and Kim (2016), this no-slip assumption does not significantly change model results relative to results generated using a frictional EPS-soil interface.

2.2 Material Properties

2.2.1 EPS Geofabric

EPS geofabric was simulated as a Linear-Elastic/Mohr-Coulomb material with post-yield strain-hardening using FLAC’s built-in Strain-Hardening/Softening Model (Itasca, 2011). Material properties for the EPS geofabric were assigned based on the density-dependent EPS constitutive model developed by Kim et al. (2018). This constitutive model estimates Young’s modulus, Poisson’s ratio, yield strength, and strain hardening behavior as functions of the single input variable of EPS density.

Density values used for this study were 12, 15, and 19 kg/m³, corresponding to EPS designations EPS12, EPS15, and EPS19 in ASTM D6817M–15 (ASTM, 2015). Note that this standard provides information on density as well as compressive resistances at axial strain levels of 1%, 5%, and 10%. However, as these density and compressive resistance values are minimum allowable, they are unlikely to be representative of actual EPS material delivered by a manufacturer and are unconservative for compressible inclusion design (i.e., relatively low stiffness values would suggest relatively high compressibility). Instead, density-dependent correlations developed by Kim et al. (2018) based on test results published by several previous researchers were used; these correlations are more likely than the ASTM D6817M–15 minimum values to be representative of EPS material encountered in practice. Equations in Table 1 were used to calculate initial Young’s modulus (E_f), Poisson’s ratio (ν_f), yield strength (τ_{yield}), and the ratio ($\tau_{10\%} / \tau_{yield}$) between shear strength at 10% axial strain and shear strength at yield for the three different EPS types (or three different EPS densities).

Table 1. Assumed properties of EPS (based on Kim et al., 2018).

EPS Parameter	Equation (ρ_f^*)
Initial Young’s modulus, E_f (MPa)	$E_f = 0.43 \rho_f - 2.60$
Poisson’s ratio, ν_f (unitless)	$\nu_f = 0.0056 \rho_f + 0.0024$
Yield strength, τ_{yield} (kPa)	$\tau_{yield} = 3.64 \rho_f - 20.66$
Ratio between shear strength at 10% axial strain and shear strength at yield, $\tau_{10\%} / \tau_{yield}$ (unitless)	$\frac{\tau_{10\%}}{\tau_{yield}} = 0.0037 \rho_f + 1.1651$

* ρ_f = EPS density in kg/m³

2.2.2 Soil

The SW, ML, and CL backfill soils (at 95% standard Proctor density) were modeled as nonlinear-elastic / Mohr-Coulomb materials. Parameter values for the backfill soils were based on those used in a numerical study by Huang et al. (2007) and those evaluated experimentally by Boscardin et al. (1990). The soil elastic behavior was controlled by a stress-dependent tangent Young’s modulus (E_t) and a stress-dependent tangent bulk modulus (K_t). These two values were evaluated according to the hyperbolic formulation described by Boscardin et al. (1990). The bulk modulus values were adjusted, if needed, to maintain a tangent Poisson’s ratio (ν_t) within the range of 0.00 to 0.49, inclusive. Input values for the three backfill soils are listed in Table 2.

Table 2. Assumed properties of backfill soil (based on Huang et al., 2007).

Soil Parameter	Value by Soil Type		
	Well-graded sands and gravelly sands (SW)	Inorganic silts or very fine sands (ML)	Inorganic clays of low to medium plasticity (CL)
Young's modulus number, K_e (unitless) ^(1,2)	950	440	120
Young's modulus exponent, n (unitless) ⁽²⁾	0.60	0.40	0.45
Failure ratio, R_f (unitless) ⁽²⁾	0.70	0.95	1.00
Initial bulk modulus number, B_i/p_a (unitless) ⁽³⁾	74.8	48.3	21.2
Asymptotic volumetric strain value, ϵ_u (unitless) ⁽³⁾	0.02	0.06	0.13
Friction angle, ϕ (degree)	48	37	17
Cohesion, c (kPa)	2	28	62
Angle of dilation, ψ (degree)	6	2	0
Total density, ρ_t (Mg/m ³)	2.25	2.03	1.90

Notes:

- (1) Multiplied by 1.1 for loading and unloading.
- (2) Calculated Young's modulus adjusted to maintain value within the range of 100 kPa to 500 MPa.
- (3) Calculated bulk modulus adjusted to maintain Poisson's ratio value within range 0 to 0.49.

2.2.3 Pipe

The pipe properties were assumed based on those used by Witthoef and Kim (2016) to simulate the laboratory-scale pipe used in the Kim et al. (2010) model-scale tests. The pipe was made of steel and had an outside diameter of approximately 10 cm. Witthoef and Kim (2016) evaluated the pipe load-response parameters by simulating a series of parallel plate / ring compression tests performed by Kim et al. (2010). Input values of Young's modulus, moment of inertia, cross-sectional area, and density of the steel pipe are summarized in Table 3.

Table 3. Assumed properties of steel pipe (based on Witthoef and Kim, 2016).

Pipe Parameter	Value
Pipe outside diameter (m)	0.1
Young's Modulus, E_{sp} (GPa)	200
Moment of Inertia, I_{sp} (m ⁴ /m)	47×10^{-12}
Cross-sectional Area, A_{sp} (m ² /m)	1.5×10^{-3}
Density, ρ_{sp} (Mg/m ³)	8

3 PARAMETRIC STUDY

A series of simulations was performed to evaluate the effects of soil type, EPS type, and EPS panel dimensions on vertical and lateral stresses around the steel pipe. This parametric study was performed in two phases. First, for each combination of soil type and EPS type, the width of the EPS panel was varied from approximately 0.6 to 2.5 times the pipe diameter, while the initial thickness of the panel was held constant at 0.5 times the pipe diameter. Second, for each soil type and EPS type combination, the width of the EPS panel was held constant at 1.5 times the pipe diameter, while the panel thickness was varied from 0.2 to 2 times the pipe diameter.

3.1 EPS Panel Width Variation with Constant Thickness

Although reduction of overburden stress on the pipe crown is an important consideration, uniformity of stresses around the pipe should be also considered to reduce the potential for ovaling deformation, as

noted by Witthoeft and Kim (2016). For this reason, it is important to evaluate the vertical and lateral stresses on the pipe and to examine how these stresses change with the width of the compressible inclusion. Variation of vertical and horizontal earth pressures on the pipe with changing width of the EPS panel are shown in Figure 2.

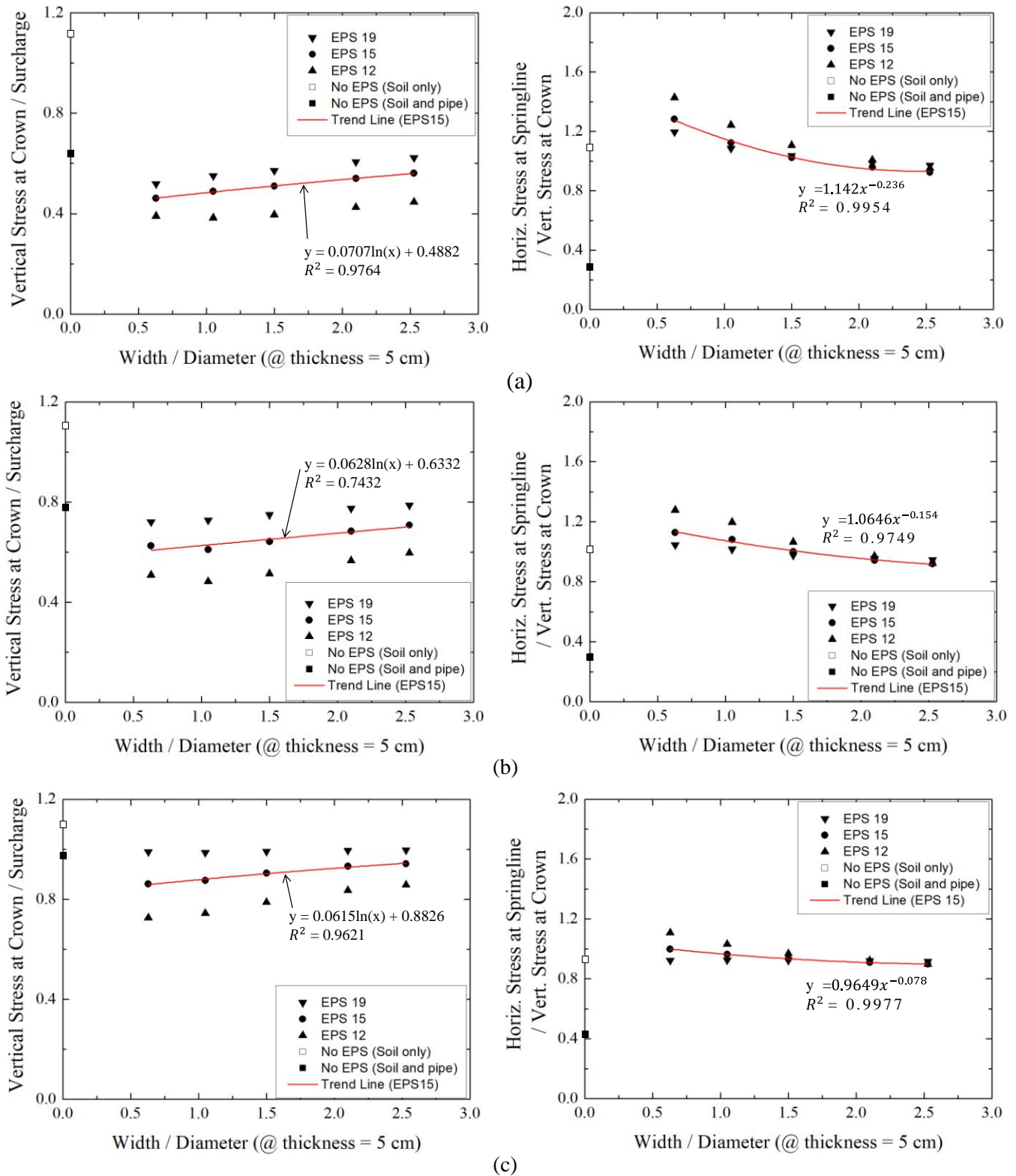


Figure 2. Variation of vertical and horizontal earth pressure at pipe crown (upper panes) with increasing width to diameter ratio for backfill soil types of (a) SW, (b) ML, and (c) CL.

Qualitatively, the results for SW soil with EPS15 (EPS density of 15 kg/m³) shown in Figures 2(a) are similar to those for SP soil with EPS15 observed by Witthoeft and Kim (2016). It is noted that the effectiveness of the EPS panel is less as the EPS density is increased (resulting in higher stiffness and

lower compressibility). For the case of CL backfill material with an EPS19 panel, the benefit of the compressible inclusion becomes almost negligible. In particular, and, apparently, regardless of soil type:

- (1) The magnitude of the vertical earth pressure is reduced by the presence of the pipe itself;
- (2) Vertical earth pressure tends toward its lowest value for a EPS panel width nearly the same as the pipe diameter and tends to increase modestly with increasing EPS panel width; and
- (3) Horizontal earth pressure tends toward its highest value for a narrow EPS panel and tends to decrease modestly with increasing panel width.

Based on the results shown in Figure 2 and the work of Witthoef and Kim (2016), an EPS panel width of approximately 1.5 times the pipe diameter provides a reasonably good compromise between reducing vertical earth pressure and maintaining uniform earth pressure around the pipe.

3.2 EPS Panel Thickness Variation with Constant Width

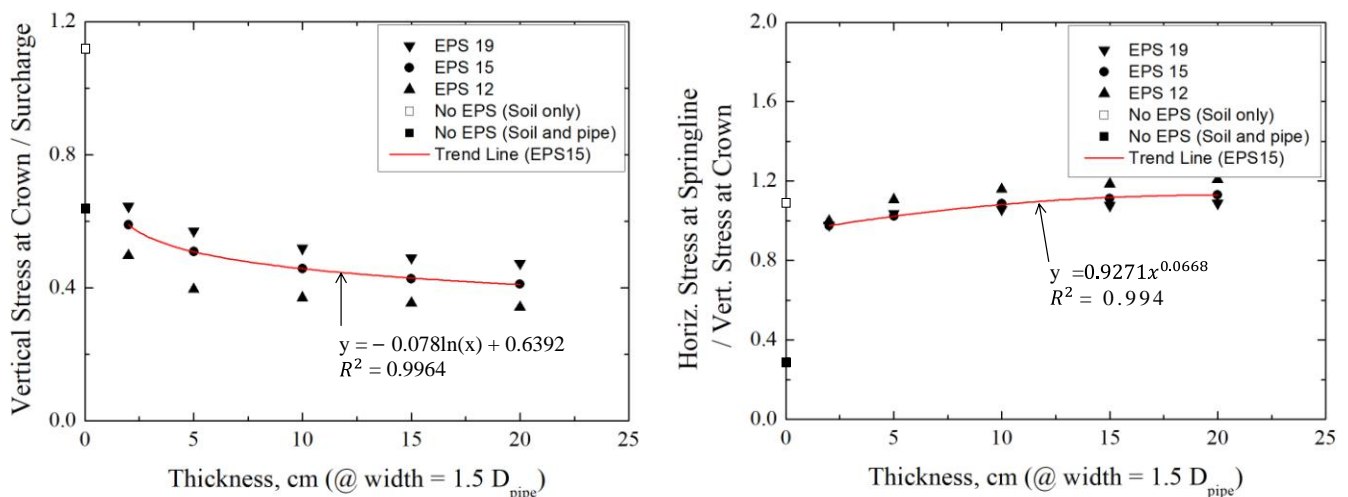
The second step of the parametric study used a constant EPS panel width of 1.5 times the pipe diameter. Although the width of the compressible inclusion over a buried pipe is typically assumed to be equal to the pipe diameter, as noted by Sladen and Oswell (1988), Witthoef and Kim (2016), and others, and as observed in the present study, the vertical load shed to either side of the pipe tends to result in increased horizontal loads at the pipe springline. This effect, which may be more or less important depending on the pipe characteristics and should be considered when using a compressible inclusion in practice, can be mitigated to some extent by widening the compressible inclusion. However, based on the “optimization” criteria suggested by Witthoef and Kim (2016) and the trends shown in Figure 2 (i.e., ratio of horizontal to vertical stress tending toward 1 with increasing panel thickness), it seems reasonable to consider a compressible inclusion width of around 1.5 times the pipe diameter.

To evaluate the effect of EPS panel thickness, a single panel width of 1.5 times the pipe diameter was selected, and the panel thickness was varied. Model-predicted variations of vertical and horizontal earth pressures with variations in EPS panel thickness are shown in Figure 3.

Qualitatively, the results shown in Figure 3 suggest the following:

- (1) The magnitude of the vertical earth pressure is reduced by a greater degree as the thickness of the EPS panel is increased;
- (2) The magnitude of the vertical earth pressure is reduced by a greater degree as the EPS density is decreased;
- (3) Horizontal earth pressure tends to increase modestly with increasing the EPS panel compressibility;
- (4) Effect (1) appears to reach a point of diminishing returns at or before a thickness of 2 times the pipe diameter; and
- (5) Effects (1) and (2) both indicate that increasing compressibility of the EPS panel results in greater reduction of vertical earth pressure.

It is noted that the effectiveness of the EPS panel is less as the EPS density increased (resulting in higher stiffness and lower compressibility). For the case of CL backfill material with an EPS19 panel, the benefit of the compressible inclusion becomes almost negligible.



(a)

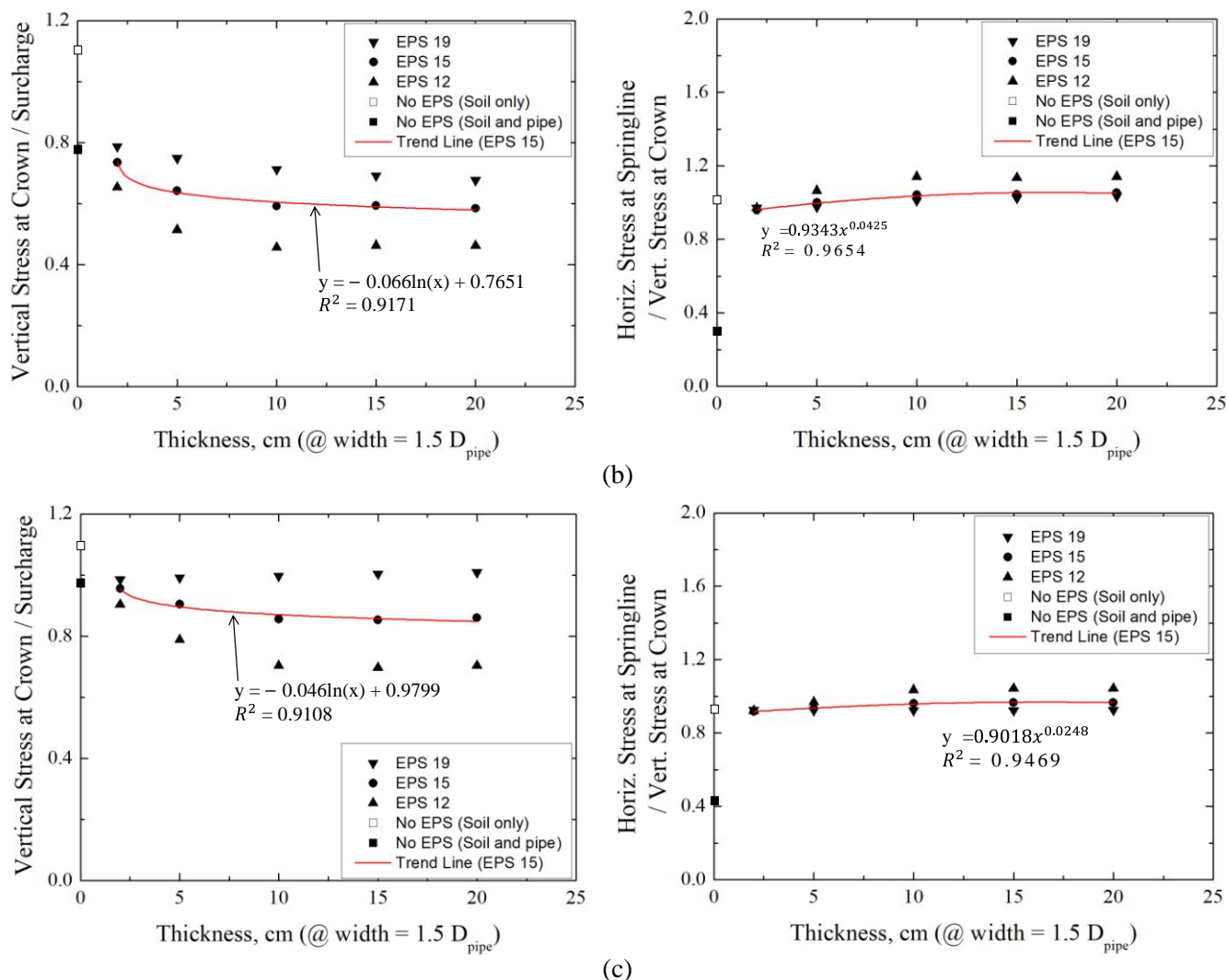


Figure 3. Variation of vertical earth pressure at pipe crown (upper panes) and horizontal earth pressure at pipe springline (lower panes) at end of surcharging phase for backfill soil types: (a) SW; (b) ML; and (c) CL.

3.3 Effective Compressibility Index

The trend shown in the upper panes of Figure 3 (i.e., decreasing vertical stress with increasing EPS panel thickness and compressibility, with diminishing returns to increased thickness) suggests that the soil arching effect over the pipe becomes more pronounced with increased displacement until full mobilization. Intuitively, the degree of mobilization of the soil arching effect is related to the ratio of settlement above the pipe to settlement outside the pipe (and compressible inclusion) footprint. This ratio is, in turn, related to the ratio of soil compressibility to inclusion compressibility.

While, for simplicity, soil compressibility is here assumed to be approximately constant for a given soil type and surcharge level, EPS panel compressibility is a function of the EPS stiffness and the panel thickness. As a means to evaluate relative compressibility of the soil and EPS panel, it is proposed to define a dimensionless *effective compressibility index*, $C_{\text{effective}}$, as follows:

$$C_{\text{effective}} = \left(\frac{E'_{\text{soil}}}{E'_{\text{EPS}}} \right) \left(\frac{t_{\text{EPS}}}{D_{\text{pipe}}} \right) \quad (1)$$

where E'_{soil} and E'_{EPS} are the constrained moduli of soil and EPS material, respectively, t_{EPS} is the thickness of the EPS panel, and D_{pipe} is the pipe diameter. For this study, the soil Young's modulus and bulk modulus were evaluated for one numerical zone near the approximate center of the test box at the maximum surcharge load for the case with soil only (i.e., no pipe and no EPS panel) and were used to calculate the constrained modulus. For the EPS panel the constrained modulus was calculated using the

initial (linear elastic) portion of the load-response path (i.e., initial Young's modulus and Poisson's ratio using the equations in Table 1).

Figure 4 shows the use of the proposed dimensionless effective compressibility index as a predictor of EPS panel effects for a panel width of 1.5 times the pipe diameter. Data in the figure were developed for SW, ML, and CL material types. As shown in the figure, there appears to be a strong correlation between the effective compressibility index and the vertical and horizontal stresses on the pipe. This finding suggests that relative stiffness is an important determinant (i.e., R^2 of 0.75 to 0.85, suggesting that 75% to 85% of the variation in these stresses can be explained by this single variable) of compressible inclusion effectiveness and that backfill soil strength is a secondary consideration.

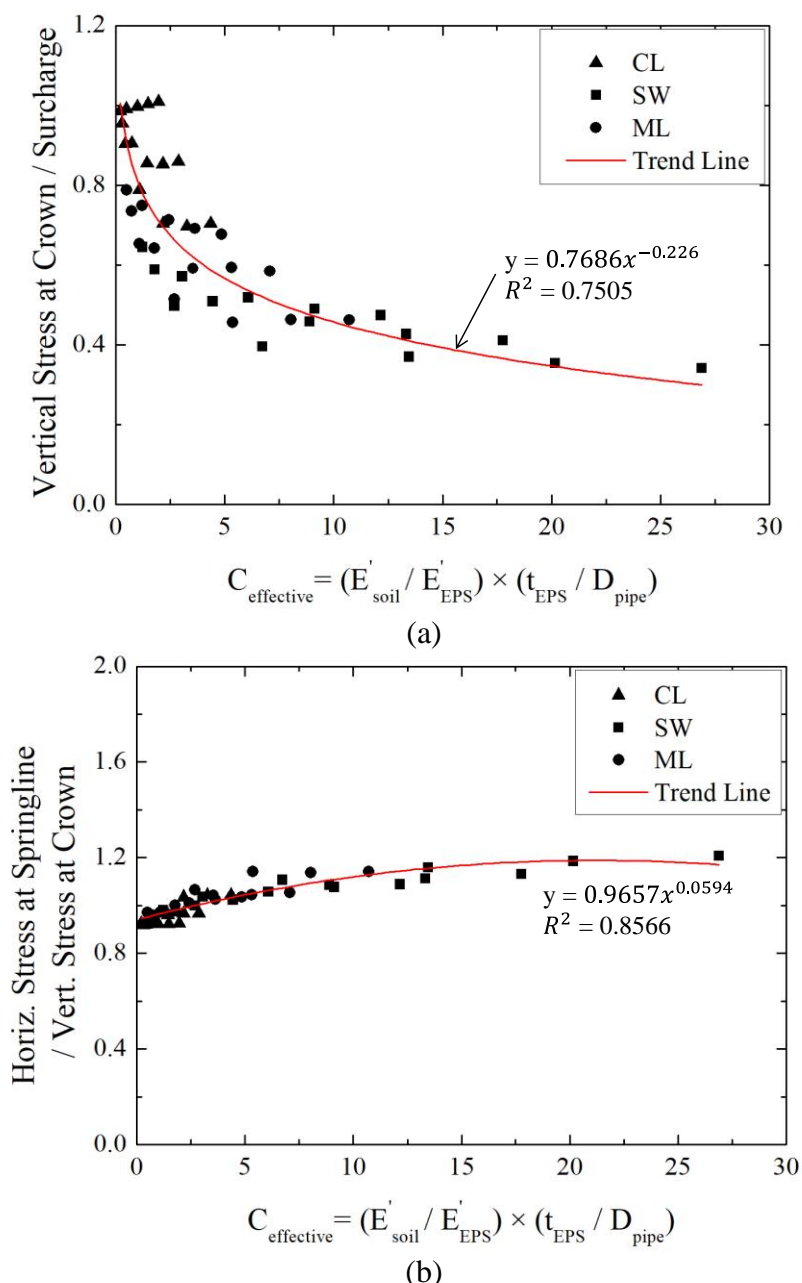


Figure 4. Illustration of the dimensionless effective compressibility index as a predictor of (a) vertical stress at the pipe crown; and (b) ratio of horizontal to vertical stress

It is noted that the combination of CL soil with EPS19 is not shown in Figure 4. As shown in Figures 2 and 3, the stress reduction achieved using EPS19 with CL is negligible. As the ratio E'_{soil} / E'_{EPS} is approximately unity for this combination, this is an unsurprising finding. Whereas the defining feature of a compressible inclusion is a significantly higher compressibility than that of the surrounding soil, by definition, an EPS panel with stiffness greater than or approximately equal to that of the surrounding soil does not effectively function as a compressible inclusion. This does not preclude use of a relatively stiff EPS panel for other functions, such as a lightweight fill material, although in such a case the stress reduction is due to the lower unit weight of the EPS, not to a positive soil arching effect.

4 SUMMARY AND RECOMMENDATIONS FOR FUTURE RESEARCH

This paper presents a numerical study to evaluate the influence of soil type and EPS type on the effectiveness of an EPS compressible inclusion used to reduce vertical earth pressure on a buried pipe. Three soil types (i.e., SW, ML, and CL at 95% standard Proctor density) and three EPS densities (i.e., EPS12, EPS15, and EPS19) are included in this numerical study.

In general, the numerical results suggest that the effectiveness of the EPS compressible inclusion can be predicted with a reasonable degree of accuracy based on the relationship between the soil and EPS stiffnesses. An *effective compressibility index* is proposed as an indicator to predict reduction of overburden stress on the pipe based on the soil stiffness and the EPS panel compressibility.

One potentially relevant design consideration is the possibility of creep in the EPS compressible inclusion. As discussed by Kim et al. (2018), creep can become significant when EPS is loaded to an axial strain of approximately 1% or more. When the plane of equal settlement is above the ground surface, settlement at the ground surface due to EPS creep might become apparent as a depression oriented along the pipe alignment. For such a condition, creep might be important an important consideration, as the surface depression could deepen and widen during the lifetime of the pipe, resulting in ongoing maintenance issues for surface features (e.g., pavement, etc.). One possible solution to this issue, as discussed by Kim et al. (2018), is to select an EPS material with the lowest density such that axial strain is 1% or less under design loads, although this would likely increase the EPS panel stiffness and reduce its effectiveness as a compressible inclusion. However, for deeply buried pipes, which likely would benefit the most from compressible inclusion use, it seems likely that the plane of equal settlement would be below the ground surface. Therefore, for most practical cases, surface expressions of creep settlement would likely be negligible.

Further research is recommended to investigate scale effects on design EPS panel thickness. For example, when specifying EPS panel thickness for a field-scale application based on laboratory-scale tests or model results, it is unclear whether EPS panel thickness should be scaled-up with pipe diameter (i.e., whether it is relevant to report in a laboratory-scale study the absolute EPS panel thickness or EPS panel thickness normalized by pipe diameter). Although it is conservative to normalized EPS panel thickness by pipe diameter, there is some evidence (e.g., Kim et al., 2010) that relatively thin EPS panels can adequately mobilize soil arching for a field-scale application, suggesting that a normalized approach might be overly conservative.

The effect of pipe stiffness is not considered in this study. Pipe stiffness should influence the earth pressure distribution on the pipe, and hence, the earth pressure reduction by compressible inclusion would change accordingly. Additionally, it is unclear whether the normalization of vertical earth pressure reduction, as is presented here, is useful or whether an absolute magnitude should be presented. For example, if the plane of equal settlement is below the ground surface, then the soil arching might be considered as fully mobilized. In that case, for a larger height of embankment fill over the pipe, the normalized earth pressure reduction would be smaller, although the magnitude of the reduction would be the same. Further efforts are recommended to compare the usefulness of normalization when reporting earth pressure reduction.

ACKNOWLEDGEMENTS

This work was supported by the Incheon National University Research in 2018–2019. The authors also thank Neven Matasovic of Geo-Logic Associates, Inc., Costa Mesa, California, for his peer review of the original manuscript and valuable comments.

REFERENCES

- AbdelSalam, S.S. and Azzam, S.A. (2016). Reduction of lateral pressures on retaining walls using geofom inclusion. *Geosynthetics International*, Volume 23, Issue 6, pp. 395–407. <https://doi.org/10.1680/jgein.16.00005>
- ASTM (2015). ASTM D6817/D6817M–15: Specification for Rigid Cellular Polystyrene Geofom. ASTM International, West Conshohocken, PA, USA.
- Athanasopoulos, G.A., Pelekis, P.C., and Xenaki, V.C. (1999). Dynamic Properties of EPS Geofom: An Experimental Investigation, *Geosynthetics International*, Volume 6, Issue 3, pp. 171–194. <https://doi.org/10.1680/gein.6.0149>

- Boscardin, M. D., Selig, E. T., Lin, R. S., and Yang, G. R. (1990), Hyperbolic parameters for compacted soils. *Journal of Geotechnical Engineering*, Vol. 116(1), pp. 88–104.
- Bartlett, S. F. and Lingwall, B. N. (2014), Protection of Pipelines and Buried Structures Using EPS Geofoam, *Geo-Shanghai 2014*, American Society of Civil Engineers, <https://doi.org/10.1061/9780784413401.054>
- Dasaka, S.M. and Gade, V.K. (2018). *Geotechnics for Natural and Engineered Sustainable Technologies: Effect of Long-Term Performance of EPS Geofoam on Lateral Earth Pressures on Retaining Walls*, Springer,
- Horvath, J. S. (1997), The compressible inclusion function of EPS geofoam, *Geotextiles and Geomembranes*, Volume 15, Issues 1–3, pp.77-120, [https://doi.org/10.1016/S0266-1144\(97\)00008-3](https://doi.org/10.1016/S0266-1144(97)00008-3)
- Huang, B., Hatami, K. and Bathurst, R. J. (2007), Parametric analysis of a 9-m high reinforced soil wall with different reinforcement materials and soil backfill, *IS-Kyushu 2007*, Fukuoka, Kyushu, Japan, 6 pp.
- Itasca. (2011). *FLAC user's manual*. Fifth Edition (FLAC Version 7.0), dated September 2011, Itasca Consulting Group, Inc., Minneapolis, Minnesota, USA.
- Kim, H., Choi, B., and Kim, J. (2010). Reduction of earth pressure on buried pipes by EPS geofoam inclusions. *Geotechnical Testing Journal*, Vol. 33(4), pp. 1-10.
- Kim, H., Witthoeft, A. F., and Kim, D. (2018) Numerical Study of Earth Pressure Reduction on Rigid Walls using EPS Geofoam Compressible Inclusions. *Geosynthetics International*, Volume 25, Issue 2, April, 2018, pp. 180-199. <https://doi.org/10.1680/jgein.18.00001>
- Marston, A. (1930). The theory of external loads on closed conduits in the light of the latest experiments. *Bulletin 96*. Iowa Engineering Experiment Station, Iowa State College, Ames, Iowa.
- Sladen, J.A. and Oswell, J.M. (1988). The induced trench method-a critical review and case history. *Canadian Geotechnical Journal*, Vol. 25, pp. 541-549.
- Witthoeft, A.F. and Kim, H. (2016). Numerical investigation of earth pressure reduction on buried pipes using EPS geofoam compressible inclusions. *Geosynthetics International*, Vol. 23(4), pp. 287-300.